electronics

MDPI

Article

Postwall-Slotline Stepped Impedance Resonator and Its Application to Bandpass Filter with Improved Upper Stopband

Liang Yang, Cheng Lu, Jialin Wang, Shunli Li, Hongxin Zhao, and Xiaoxing Yin *

State Key Laboratory of Millimeter Waves, Southeast University, Nanjing 210096, China;
lyangween@live.com (L.Y.); 15952039133@126.com (C.L.); wjlbaoyan@163.com (J.W.);
lishunli621@seu.edu.cn (S.L.); zhaohongxin@seu.edu.cn (H.Z.)
* Correspondence: xxyin@seu.edu.cn

Abstract: In this letter, a postwall-slotline stepped impedance resonators (PWS-SIR) is proposed and applied to a bandpass filter (BPF) with a wide stopband. The proposed PWS-SIR-BPF is composed of three U-shaped PWS-SIRs and two microstrip-slot feeding transitions. A PWS has a much lower impendence which a conventional slotline (CSL) cannot reach, so that a much smaller impendence ratio of the PWS-SIR can be achieved. Consequently, a wider stopband simultaneously can be realized for the proposed filter. The designed PWS-SIR-BPF, as well as a CSL-BPF, have been fabricated, measured and compared to verify the features of the PWS-SIR. The measured results are consistent with the simulation ones. The PWS-SIR is 7.3 mm ($0.22\lambda_0$) long, which is 67% of 11.1 mm ($0.34\lambda_0$) of the CSL resonator. The first spurious resonance frequency of the PWS-SIR-BPF is extended from 9.8 GHz ($2f_0$) to 23 GHz ($4.7f_0$).

Keywords: Miniaturization bandpass filter, postwall slotline, stepped impendence resonators.

1. Introduction

Bandpass filter (BPF) based on slotline has been widely applied in modern wireless communication systems [1]-[5]. Due to its semi-open structure, a conventional slotline (CSL) BPF suffers from large sizes, and narrow stopband. Ones employed a loading strip on the slotline to miniaturize its overall size and realize a wide upper stopband [6][7]. A double-spiral slotline resonator is utilized to make the filter more compact [8],[9].

A stepped impedance resonator (SIR) is a powerful way to a compact size and as well as wide stopband filters [10-19]. The lower the impedance ratio of SIR is, the smaller the size is and wider the stopband is. However, implementing SIR with CSL is difficult and not effective, because a CSL cannot reach a low impedance so that CSL-SIR cannot also reach a low impedance ratio.

In this letter, a postwall-slotline stepped impedance resonators (PWS-SIR) is proposed and applied to a bandpass filter (BPF) with a wide stopband. Due to much lower impendence of a PWS [12], the proposed postwall slotline stepped impedance resonator (PWS-SIR) can achieve a lower impendence ratio with a smaller size. Thus, the features of compact and wide stopband of the SIR-BPF can be realized with PWS. The designed PWS-SIR-BPF, as well as a CSL-BPF, have been fabricated, measured and compared. The PWS-SIR is 7.3 mm ($0.22\lambda_0$) long, which is 67% of 11.1 mm ($0.34\lambda_0$) of the CSL resonator. The PWS-SIR-BPF has a very wide stopband rejection of up to $4.7f_0$ while the stopband of the CSL-BPF is just up to $2f_0$, and it also has better rectangular factor and selectivity.

2. Filter Design

2.1. Filter Structure

Figure 1 presents the proposed BPF. The designed BPF is a two-layer printed circuit board and fed by a microstrip-slot structure. The three U-shaped PWS resonators are printed on the both sides of the substrate and two microstrip lines are placed on the top layer for feeding, as is shown in Figure 1(c) and (d). PWS is a slot-based transmission line with two rows of metalized via connecting the top strip and bottom plane on either side of CSL [20]. The $\lambda_g/2$-type stepped impedance resonator (SIR) is composed by a PWS and a CSL. The high impendence portion of the SIR, which is presented in Figure 1(a), is a CSL with 2 mm slot width and the low impendence portion is a PWS with 0.2 mm slot width.

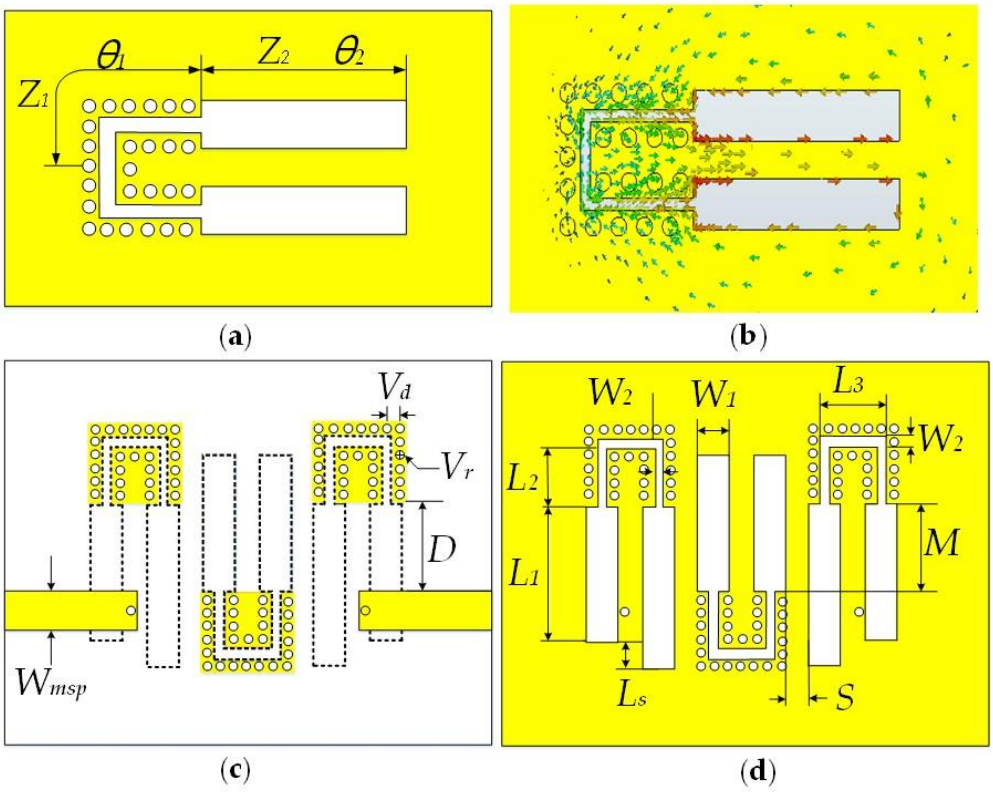


Figure 1. The proposed BPF. (**a**) The SIR composed of PWS, (**b**) the current distribution at the resonance frequency, (**c**) the top view, (**d**) the bottom view, W_{msp}=1.1 mm, V_d=0.6 mm, V_r=0.15 mm, D=2.7 mm, M=2.9mm, L_1=4.02 mm, L_2=2 mm, L_3=1.6 mm, L_s=0.85 mm, W_1=2 mm, W_2=0.2 mm, S=0.6 mm.

2.2. PWS-SIR Resonator

As shown in Figure 1(a), the characteristic impendence and electrical length of PWS are defined as Z_1 and θ_1. Similarly, the characteristic impendence and electrical length of CSL are Z_2 and θ_2. Besides, the impedance ratio of SIR, defined as K=Z_1/Z_2, is less than 1.00. According to the theory of the SIR [21], when the SIR is resonating, K_{pws} and electrical length can be expressed as follows

$$K_{pws} = \frac{Z_1}{Z_2} = \tan\theta_1 \times \tan\theta_2 < 1 \quad (1)$$

$$\theta_1 + \theta_2 < \frac{\pi}{2} \quad (2)$$

The resonator can get a minimum electrical length which is less than the half of wavelength when θ_1 and θ_2 are equivalent, thus achieving the miniaturization of the resonators.

The characteristic impedance of PWS and CSL can be calculated by the full wave EM simulator ANSOFT HFSS. The characteristic impedance of PWS cannot be achieved like

CSL because it is not a uniform transmission line. The characteristic impedance of the PWS can be calculated by the ABCD matrix, which is used to calculate the characteristic impedance of the periodic structure unit [22]. The characteristic impedance of CSL with a 2 mm gap at the Rogers RO4003C of 0.508 mm thickness is 215 ohm and the characteristic impedance of the PWS with 0.20 mm gap is 43.88 ohm. The characteristic impendence of CSL and PWS with different slot width is calculated, as is shown in Figure 2, and the PWS under the same slot width has a smaller impendence than CSL. The PWS adopted for implementing SIR, as is shown in Figure 1(a), can result in a smaller impendence ratio K_{pws} and thus a smaller size than CSL-SIR. The impendence ratio K_{pws} and the miniaturization ratio of the proposed resonator are 0.20, 0.62, respectively.

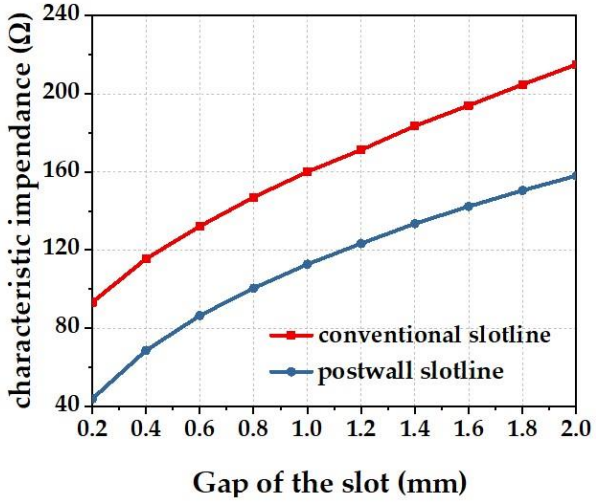


Figure 2. Characteristic impedance of the PWS and the conventional slotline.

For the filter, the location of the spurious passband is directly related to the performance of the filter and the spurious passband theory of CSL-SIR is well established [9]. Taking the spurious resonance frequency to be f_n (n=1, 2, 3...) and corresponding electrical length with θ_n and then the following relation can be achieved

$$\frac{f_1}{f_0} = \frac{\theta_1}{\theta_0} = \frac{\pi}{2\tan^{-1}\sqrt{K_{pws}}} \tag{3}$$

where the f_0 is the fundamental frequency of the PWS-SIR. Obviously, the spurious passband frequency of the resonator is determined by the impendence ratio K_{pws}. The spurious passband can be postponed with a smaller impendence ratio K_{pws}. Based on the above discussion, the SIR based on PWS structure can achieve a smaller impendence ratio than CSL-SIR, leading to a higher spurious passband. According to (3), the frequency of the first spurious response of the proposed resonator is as follows

$$f_1 = \frac{\theta_1}{\theta_0} f_0 = \frac{\pi}{2\tan^{-1}\sqrt{K_{pws}}} f_0 = 3.71 f_0 \tag{4}$$

The unloaded Q-factor of the resonator have a great influence on the insertion loss of the filter. To compare the unloaded Q-factor of PWS-SIR and CSL-SIR, the loss of these resonators when they resonate at 4.9 GHz with the same feeding structure is simulated, as is shown in Table 1. It can be seen that the radiation loss of the PWS-SIR is smaller, which is 55.6 percent of the radiation loss of the CSL-SIR. Due to the closed field distribution of the PWS, more electric field is concentrated in the substrate. Thus, the radiation loss and the crosstalk to other devices of the PWS-SIR is smaller. This means the PWS has a higher unloaded Q-factor.

Table 1. The Loss Percentage of Two Resonator.

	Conductor loss (%).	Dielectric loss(%)	Radiation loss(%)	Total loss(%)
PWS-SIR	0.594	0.604	7.215	8.410
CS-SIR	0.553	0.572	12.975	14.095

2.3. Filter Design

A third-order filter with a bandwidth BW=200 MHz centered at f_0 =4.9 GHz is implemented with the proposed PWS-SIR structure. Coupling matrix and external Q-factor are obtained from CST filter design tool. The obtained external Q-factor is 13.93 and the coupling matrix is as follows

$$m = \begin{bmatrix} 0 & 0.042 & 0 \\ 0.042 & 0 & 0.042 \\ 0 & 0.042 & 0 \end{bmatrix} \quad (5)$$

For the dimensions of the resonator designed as shown in Figure 1, the proposed resonator resonates at 4.9 GHz. Obviously, based on the proposed resonator's current distribution in Figure 1(b), the current of the U-shaped resonator is the largest at the slot end and the currents of the two terminals flow opposite direction. The cancellation currents greatly reduces the radiation loss of the resonator and consequently a higher unloaded Q-factor is achieved.

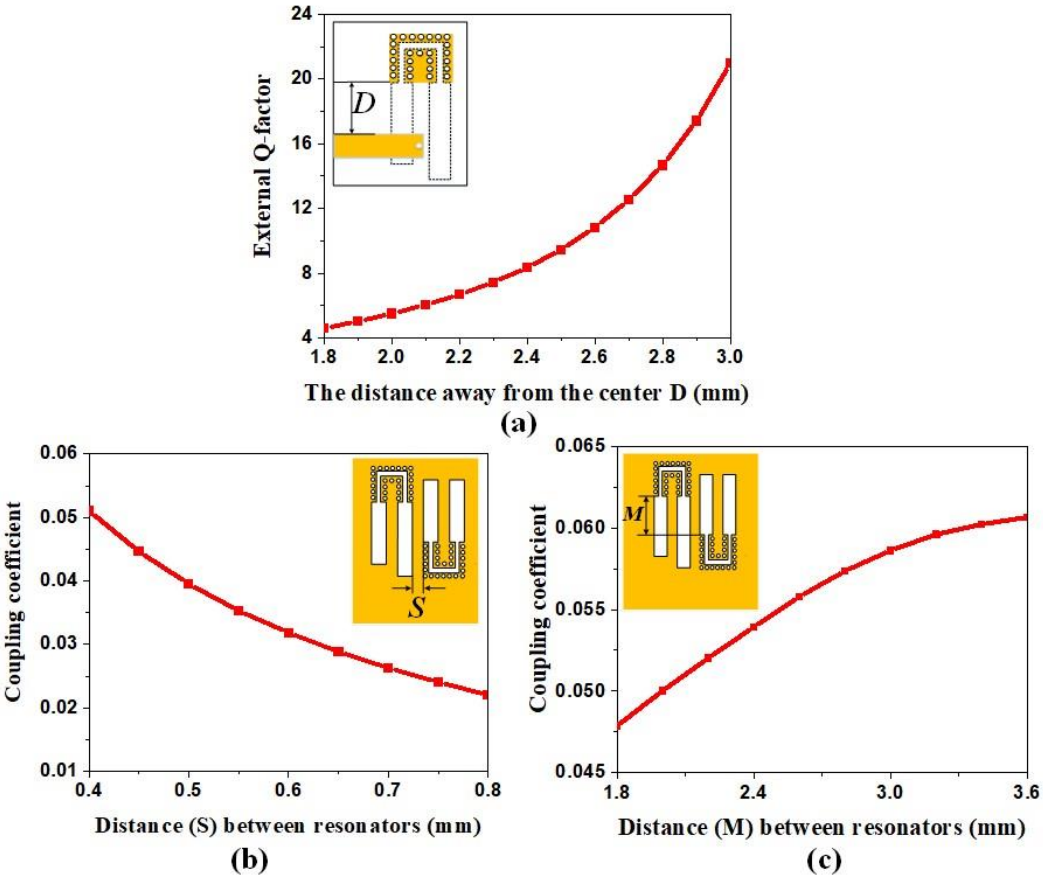


Figure 3. External Q-factor and coupling coefficients of the PWS filter.

The distance between the microstrip line and the center of the board D affects the external Q-factor and the relationship curve is shown in Figure 3(a). The coupling coefficient of the filter depends on the distance between the resonators S and M. The relationship between the distance and the coupling coefficient have been obtained by simulation in CST, as presented in Figure 3(b) and (c).

According to the results in Figure 3, S, M and D can be optimized to satisfy the coupling coefficient and external Q-factor which has been calculated theoretically. To compensate the influence of the feeding microstrip on the resonator, the length of the first and the last resonator need to increase L_s (0.85 mm). The CSL filter using for comparison is also designed in the same way.

3. Fabrication and Measurement Results

The proposed PWS and CSL filters have been designed, fabricated and measured. Figure 4 shows the photo of the two filters. The two filters are fabricated on the same RO4003C substrate of 0.508 mm thickness, whose dielectric constant is 3.38, and a microstrip line is also made on the board for calculating the insertion loss of the connector and microstrip line approximately. The length of the CSL filter resonator is 11.1 mm ($0.34\lambda_g$), and the length of the proposed filter resonator is just 7.3 mm ($0.22\lambda_g$), which is 35% smaller than the CSL filter.

The two filters are measured by a Keysight N5224A vector network analyzer and the measured results of both filters are shown in Figure 5. The measured passband insertion loss of the PWS filter and the CSL filter are both 1.7 dB, which are in good agreement with the simulated ones. In Figure 5 (b), the stopband rejection of the PWS filter is better than -20 dB from 5 GHz to 23 GHz, which shows that the PWS filter has a very wide stopband rejection of up to $4.7f_0$. The stopband of the CSL is just up to 10 GHz ($2\ f_0$), as is shown in Figure 5 (a). And it can be noted that the suppression of the spurious passband predicted at $3\ f_0$ is better than 25 dB. As a result, at the same passband bandwidth, the proposed filter not only has a small size, but also has a wide upper stopband. The insertion loss and the upper stopband rejection comparisons of the conventional slotline filter and the PWS-SIR filter at normalized frequency are shown in Figure 6 (a) and (b). The results show that the wideband rejection of the PWS-SIR-BPF is improved definitely with similar insertion loss. A comparison table with state-of-the-art of slotline filters is shown in Table 2.

Table 2. Comparison Of The Slotline Filters With State-Of-The-Art.

	F_0/GHz	**Insertion loss/dB**	**Size/λ_0**	**Upper Stopband (>20dB)/GHz**	**Upper Stopband (>20dB) /f_0**
[6]	3	0.67	0.55*0.8	To 7	2.30
[7]	2.44	2	0.152*0.206	To 16 > 18dB	6.55 > 18dB
[9]	2.11	2	0.078*0.087	To 5	2.37
[10]	1.5	3	0.78*0.14	To 12.5	8.3
[11]	2.5	2	1.04*0.39	To 16	6.4
[12]	1.51	2.7	0.32*0.22	To 12.5	8.3
[13]	1.549	2.723	0.18*0.07	To 30	19.4
[14]	2.48	1.1	0.74*0.17	To 30	12.1
[15]	1.5	2.52	0.16*0.12	To 17	11.3
[16]	2.4	2.4	0.13*0.08	To 22.5	9.4
[17]	0.4	0.5		To 3.4	8.5
This work	4.9	1.7	0.22*0.22	To 23	4.7

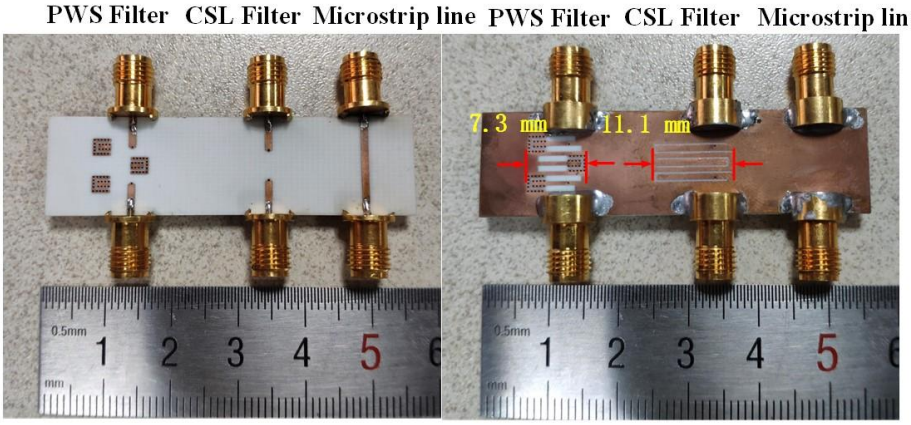


Figure 4. The photo of the proposed BPF. (**a**) the top view of the BPF board, (**b**) the bottom view of the BPF board.

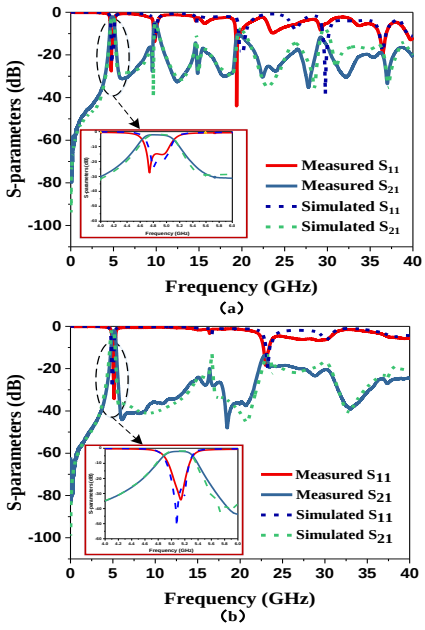
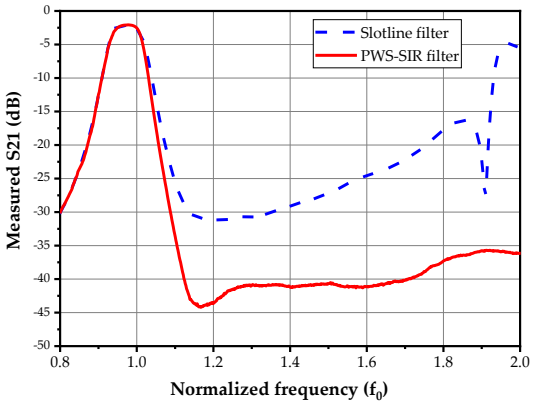
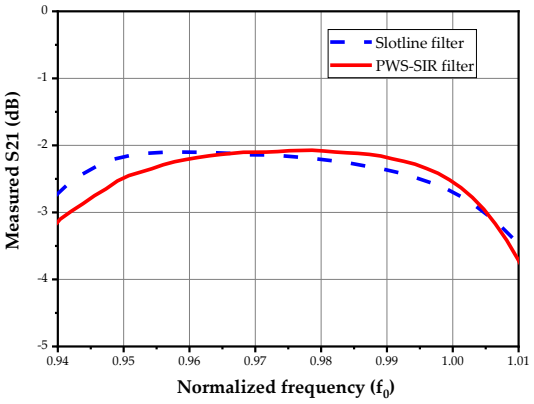


Figure 5. Comparison between simulation and measurement of both BPF. (**a**) CSL filter, (**b**) PWS filter.



(**a**)



(**b**)

Figure 6. The insertion loss (**a**) and the upper stopband rejection (**b**) comparisons of the conventional slotline filter and the PWS-SIR filter at normalized frequency.

4. Conclusions

To conclude, a third-order BPF based on PWS-SIR have been proposed and designed in this letter. Besides, the advantages of PWS-SIR compared with CSL-SIR are also explained. The measured results are consistent with simulated results. The proposed BPF not only realizes the miniaturization of the slotline BPF but also makes the stopband wider in comparison with the conventional slotline filter. The results demonstrate that the PWS-SIR filter has a wider application than the CSL filter.

Author Contributions: Conceptualization, S.L., H.Z., and X.Y.; Methodology, L.Y., C.L. and J.W.; Validation, L.Y.; Formal analysis, L.Y.; Data curation, C.L. and J.W.; Writing-original draft preparation, L.Y.; Writing-review and editing, C.L. and J.W.; Supervision, S.L., H.Z., and X.Y.; Project administration, S.L., H.Z., and X.Y. All authors have read and agreed to the published version of the manuscript.

Funding: This research was funded by National Natural Science Foundation of China under Grant 61801116 and 61771127.

References

1. M. K. Mandal and S. Sanyal, "Compact wide-band bandpass filter using microstrip to slotline broadside-coupling," *IEEE Microw. Wireless Compon. Lett.* **2007**, *vol. 17*, no. 9, pp. 640-642.
2. S. K. Remillard, P. O. Radzikowski, S. Cordone, D. S. Applegate, A.Mehrotra, J. D. Kokales, and A. Abdelmonem, "A closed slot-line resonator filter," *IEEE Microw. Wireless Compon. Lett.* **2004**, *vol. 14*, no. 5, pp.234–236.
3. S. Sun and W. Menzel, "Novel dual-mode balun bandpass filters usingsingle cross-slotted patch resonator," *IEEE Microw. Wireless Compon. Lett.* **2011**, *vol. 21*, no. 8, pp. 415–417.
4. V. K. Killamsetty and B. Mukherjee, "Compact Wideband Bandpass Filter for TETRA Band Applications," *IEEE Microw. Wireless Compon. Lett.* **2017**, *vol. 27*, no. 7, pp. 630-632.
5. V. K. Killamsetty and B. Mukherjee, "Miniaturised highly selective wide-band bandpass filter using dual-mode resonators and inter digital capacitors," *Electron. Lett.* **2017**, *vol. 53*, no. 17, pp. 1209-1211.
6. L. P. Feng and L. Zhu, "Strip-loaded slotline resonator for compact differential-mode bandpass filters with improved upper stopband performance," *IEEE Microw. Wireless Compon. Lett.* **2017**, *vol.27*, no.2, pp.108-110.
7. X. Luo and J-G. Ma, "Compact Slot-Line Bandpass Filter Using Backside Microstrip Open-Stubs and Air-Bridge Structure for Spurious Suppression," Asia Pacific Microwave Conference, Singapore, 2009.
8. R. Azadegan and K. Sarabandi, "Miniature high-Q double-spiral slot-line resonator filters," *IEEE Trans. Microw. Theory Techn.* **2004**, *vol. 52*, no. 5, pp. 1548–1557.
9. J. Lee and K. Sarabandi, "A miniaturized conductor-backed slot-line resonator filter with two transmission zeros," *IEEE Microw. Wireless Compon. Lett.* **2006**, *vol. 16*, no. 12, pp. 660–662.

10. J.-T. Kuo and E. Shih, "Microstrip stepped impedance resonator bandpass filter with an extended optimal rejection bandwidth," *IEEE Trans. Microw. Theory Techn.* **2003**, *vol. 51*, no. 5, pp. 1554–1559.
11. T. Lopetegi, M. A. G. Laso, F. Falcone, F. Martin, J. Bonache, J. Garcia, L. Perez-Cuevas, M. Sorolla, and M. Guglielmi, "Microstrip"Wiggly-Line" bandpass filters with multispurious rejection," *IEEE Microw. Wireless Compon. Lett.* **2004**, *vol. 14*, no. 11, pp. 531–533.
12. C.-F. Chen, T.-Y. Huang, and R.-B. Wu, "Design of microstrip bandpass filters with multiorder spurious-mode suppression," *IEEE Trans. Microw. Theory Techn.* **2005**, *vol. 53*, no. 12, pp. 3788–3793.
13. S. C. Lin, T. N. Kuo, Y. S. Lin, and C. H. Chen, "Novel coplanar-waveguide bandpass filters using loaded air-bridge enhanced capacitors and broadside-coupled transition structures for wideband spurious suppression," *IEEE Trans. Microwave Theory and Techn.* **2006**, *vol. 54*, no. 8, pp.3359–3369.
14. X. Luo, J.-G. Ma, E.-P. Li, and K. Ma, "Hybrid microstrip T-Stub/defected ground structure cell for electromagnetic interference bandpass filter design," *IEEE Trans. Electromagn. Compat.* **2011**, *vol. 53*, no. 3, pp. 717–725.
15. C. Kim and K. Chang, "Wide-stopband bandpass filters using asymmetric stepped-impedance resonators," *IEEE Microw. Wireless Compon. Lett.* **2013**, *vol. 23*, no. 2, pp. 69–71.
16. P. Chu, W. Hong, L. Dai, H. Tang, Z. Hao, J. Chen, and K. Wu, "Wide stopband bandpass filter implemented with spur stepped impedance resonator and substrate integrated coaxial line technology," *IEEE Microw. Wireless Compon. Lett.* **2014**, *vol. 24*, no. 4, pp. 218–220.
17. J. Malherbe, "Wideband bandpass filter with extremely wide upper stopband," *IEEE Trans. Microw. Theory Techn.* **2018**, *vol. 66*, no. 6, pp. 2822–1559.
18. M. Makimoto and S. Yamashita, "Bandpass filter using parallel coupled stripline stepped impedance resonator," *IEEE Trans. Microw. Theory Techn.* **1980**, *vol. 28*, no. 12, pp. 1413–1417.
19. C. F. Chen, T. Y. Huang, and R. B. Wu, "Design of microstrip bandpass filters with multiorder spurious-mode suppression," *IEEE Trans. Microw. Theory Techn.* **2005**, *vol. 53*, no. 12, pp. 3788–3793.
20. Shunli Li, Xiaoxing Yin, Hongxin Zhao, and Hongye Qi, "Postwall slotline and its application in design of short-pulse tapered slot antennas," *IEEE Trans. Antennas Propag.* **2015**, *vol. 63*, no. 8, pp. 3400-3409.
21. M. Sagawa, M. Makimoto, and S. Yamashita, "Geometrical structure and fundamental characteristics of microwave stepped-impedance resonators," *IEEE Trans. Microw. Theory Techn.* **1997**, *vol. 45*, no. 7, pp. 1078-1085.
22. Pozar, D. M., *Microwave Engineering*, John Wiley & Sons, 2009, pp. 320-322.